

**UNIVERSITY OF SÃO PAULO  
SÃO CARLOS SCHOOL OF ENGINEERING**

**Gabriel José Negrelli Gomes**

**Development of Software for Wind Power System Model  
Identification**

**São Carlos**

**2019**



**Gabriel José Negrelli Gomes**

**Development of Software for Wind Power System Model  
Identification**

Dissertation submitted to the São Carlos  
School of Engineering of the University of  
São Paulo in partial fulfillment of the require-  
ments for the degree of Master of Science in  
Electrical Engineering.

Area: Electrical Power Systems

Supervisor: Prof. Dr. Elmer Pablo Tito Cari

**São Carlos  
2019**

## ABSTRACT

GOMES, G. J. N. **Model for theses and dissertations in  $\text{\LaTeX}$  using the USPSC class to the EESC.** 2019. 34p. Dissertation (Masters) - São Carlos School of Engineering, University of São Paulo, São Carlos, 2019.

This project proposes the development of a software for identification of wind power plant equivalent models. To do so, a generic model well-known in the literature, capable of representing wind power plants during both steady-state and transients, was chosen. The method applied to identify the model is composed of two optimization algorithms. At the beginning of the process, an heuristic approach based on Mean-Variance Mapping Optimization is used in order to reduce the parameter's search region around a possible solution. Afterward, a non-linear algorithm based on Trajectory Sensitivity is used to determine the local minimum and estimate the parameters. The method validation will be made using data from simulated systems. Also, a guided user interface will be developed for this application, aiding new users. All coding for this project will be made in Python.

**Keywords:** Wind power plants. Parameter estimation. MVMO. Trajectory sensitivity. Python.

## RESUMO

GOMES, G. J. N. **Development of Software for Wind Power System Model Identification.** 2019. 34p. Dissertation (Masters) - São Carlos School of Engineering, University of São Paulo, São Carlos, 2019.

O presente trabalho propõe o desenvolvimento de um *software* para identificação de um modelo equivalente de parques eólicos. Para este objetivo foi um modelo genérico da literatura capaz de representar de forma adequada o comportamento da planta eólica durante regime permanente e transitórios. O método utilizado para a identificação do modelo é constituído por dois algoritmos de otimização. Primeiramente, é empregada uma abordagem heurística, baseada em Otimização por Mapeamento de Média-Variância, a fim de reduzir a região de busca dos parâmetros em torno de uma possível solução. Em seguida, utiliza-se um algoritmo não-linear, baseado no Método de Sensibilidade de Trajetória, para determinar o mínimo local e estimar os valores dos parâmetros com mais precisão. A validação do método será feita utilizando medidas de sistemas simulados. Com o intuito de facilitar a experiência do usuário com o programa, será desenvolvida uma interface gráfica amigável para o *software*. Tanto as rotinas para identificação de modelos quanto a interface gráfica serão desenvolvidas em Python.

**Palavras-chave:** Plantas eólicas. Estimação de parâmetros. MVMO. Sensibilidade de trajetória. Python.



## LIST OF FIGURES

Figure 1 – Share of electricity demand in the EU covered by wind energy during 2018	12
Figure 2 – Electricity generation in Brazil by source . . . . .	13
Figure 3 – Wind and water regime in the Brazilian Northeast Region . . . . .	13
Figure 4 – Representation of Type-1 Wind Turbine Generator . . . . .	16
Figure 5 – Representation of Type-2 Wind Turbine Generator . . . . .	16
Figure 6 – Torque-speed curve . . . . .	17
Figure 7 – Representation of Type-3 Wind Turbine Generator . . . . .	18
Figure 8 – Representation of Type-4 Wind Turbine Generator . . . . .	18
Figure 9 – Share of installed capacity for each wind turbine generator type . . . .	19
Figure 10 – Type-3 WTG model proposed by Erlich . . . . .	19
Figure 11 – Flowchart of estimation method . . . . .	24
Figure 12 – Exemplification of MVMO process . . . . .	25
Figure 13 – Example of MVMO mapping function . . . . .	26
Figure 14 – Effect of different mean and shape factor values on the mapping function	27
Figure 15 – Comparison between symmetrical and asymmetrical shape factors . . .	27
Figure 16 – Results of method for spring-mass system . . . . .	31





## LIST OF ABBREVIATIONS AND ACRONYMS

ABEEólica	Brazilian Wind Energy Association
ANEEL	Brazilian Electricity Regulatory Agency
DFIG	Doubly Fed Induction Generator
EESG	Electrical Excited Synchronous Generator
EU	European Union
GUI	Graphical User Interface
IEEE	Institute of Electrical and Electronics Engineers
MVMO	Mean-Variance Mapping Optimization
PMSG	Permanent Magnet Synchronous Generator
PROINFA	Program of Incentive to Alternative Electric Energy Sources
SCIG	Squirrel Cage Induction Generator
TSM	Trajectory Sensitivity Method
US	United States of America
UK	United Kingdom
WECC	Western Electricity Coordinating Council
WRIG	Wound Rotor Induction Generator
WTG	Wind Turbine Generator



## CONTENTS

<b>1</b>	<b>INTRODUCTION</b>	<b>11</b>
<b>1.1</b>	<b>Wind Energy</b>	<b>11</b>
<b>1.2</b>	<b>Research Goals</b>	<b>14</b>
<b>2</b>	<b>MODELLING OF WIND TURBINE GENERATORS</b>	<b>15</b>
<b>2.1</b>	<b>Generic Models of Wind Turbine Generators</b>	<b>15</b>
2.1.1	Type-1 Wind Turbine Generator	15
2.1.2	Type-2 Wind Turbine Generator	16
2.1.3	Type-3 Wind Turbine Generator	17
2.1.4	Type-4 Wind Turbine Generator	17
<b>2.2</b>	<b>Model of Wind Turbine Generator Selected</b>	<b>18</b>
<b>3</b>	<b>PARAMETER ESTIMATION PROCESS</b>	<b>23</b>
<b>3.1</b>	<b>Mean-Variance Mapping Optimization</b>	<b>24</b>
<b>3.2</b>	<b>Trajectory Sensitivity Method</b>	<b>27</b>
<b>4</b>	<b>SOFTWARE CONCEPT</b>	<b>29</b>
<b>5</b>	<b>EXPECTED RESULTS</b>	<b>31</b>
<b>5.1</b>	<b>Partial Results</b>	<b>31</b>
<b>5.2</b>	<b>Work Progress</b>	<b>31</b>
	<b>BIBLIOGRAPHY</b>	<b>33</b>



## 1 INTRODUCTION

During the last decade, the world has seen an increase in participation of renewable sources in power generation, leaded mainly by wind and solar energy. These green technologies provide an alternative to sources based on fossil fuel, lowering pollution levels and reducing greenhouse gas emissions. On the other hand, the power output from these sources rely on weather conditions and can't be fully controlled.

This increase is seen worldwide, as part of policies to reduce the human impact on climate and the environment. This 'renewable wave' is leaded mainly by European countries, specially in the European Union (EU), United States (US) and China. In particular, EU has set in 2010 a strategy plan to reduce its greenhouse emissions by at least 20% compared to 1990 levels and increase the share of renewable sources to at least 20% by 2020 ([Commission European, 2010](#)).

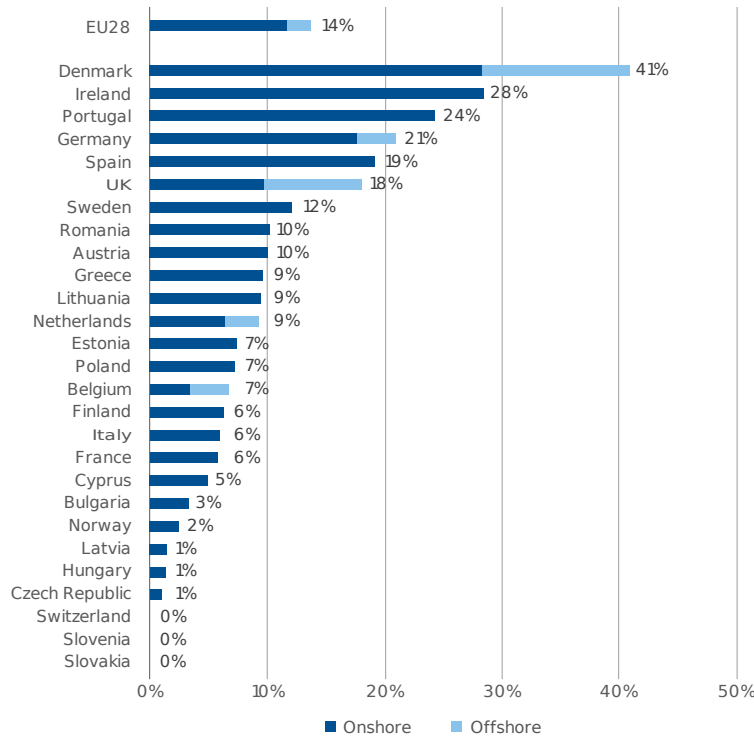
Brazil does not lag far behind EU regarding renewable sources policies. In 2002, the country passed a bill that, among other actions, creates the Program of Incentive to Alternative Electric Energy Sources (PROINFA). This program aims to increase the share of wind, solar, small hydro and biomass energy production. The final goal is to have these energy sources corresponding to 10% of Brazil's annual energy consumption by 2024 ([Federative Republic of Brazil, 2002](#)).

### 1.1 Wind Energy

Those policies stimulated the increase of wind energy participation, reaching a scenario where it is the main energy source of some countries. In the EU, wind energy alone generated 362 TWh in 2018, covering 14% of the electricity demand, a share 2% higher than 2017. Among the EU countries, Denmark leads in this sector, with 41% of its demand supplied by wind power plants, followed by Ireland (28%), Portugal (24%) and Germany (21%). The total installed capacity across the 28 EU countries is 178.8 GW, with Germany in first position, with a total installed capacity of 59.3 GW, followed by Spain and the United Kingdom (UK), with 23.5 and 21.0 GW installed, respectively ([Wind Europe, 2019](#)). Figure 1 displays the detailed percentage of electricity demand covered by wind in the EU.

In Brazil, wind energy contributed with 42.4 TWh during 2017, resulting in a participation share of 7.2%. For comparison, Itaipu, the largest power plant in Brazil, has produced 96.4 TWh during the same period. But, while other sources, such as hydro and coal, had its share lowered, wind energy had the highest variation among sources comparing to 2016, increasing its contribution by 26.5% ([EPE, 2018](#)).

Figure 1: Share of electricity demand in the EU covered by wind energy during 2018



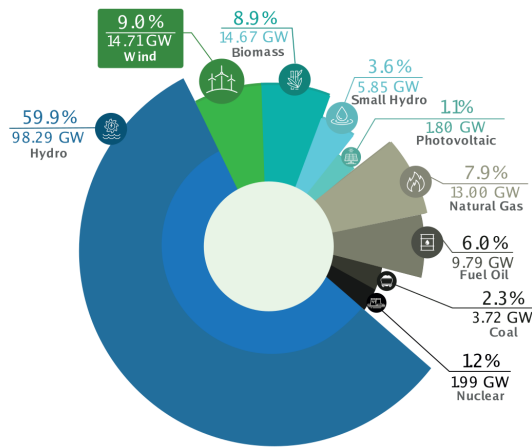
Source: Wind Europe, 2019

In terms of installed capacity, wind power plants appear in 2<sup>nd</sup> place, with 14.7 GW installed, only behind hydro power plants ([ABEEOLICA, 2018](#)), as shown in Figure 2. However, there is still plenty of energy yield for this source to be explored. In ([AMARANTE et al., 2001](#)) is shown that Brazil has potential to generate 272.2 TWh per year, with an installed capacity of 143.5 GW. The Northeast Region has the higher potential, with an annual energy yield of 144.3 TWh and potential to host up to 75.0 GW. Also, the wind regime in the Northeast Region is complimentary to the water regime of the main river responsible to power generation in the region, as presented by Figure 3. This characteristic would help controlling reservoir water level during dry season, an important resource not only for power generation, but also irrigation of crops and water supply ([ANEEL, 2005](#)).

With all this information in hand, it is only reasonable to assume that wind energy will increase its participation in electricity generation. However, some aspects of the wind energy must be considered prior to the implementation on large scale of wind power plants.

The main difficulties are due to the nature of the energy source and the generator's characteristics. The wind regime is not constant and evenly distributed across the country, depending on the region's geography and vegetation. This results in a energy source that is not entirely reliable and concentrated on a certain area. Wind turbine generators usually have their rotor decoupled from the grid via frequency converter, leading to their low

Figure 2: Electricity generation in Brazil by source

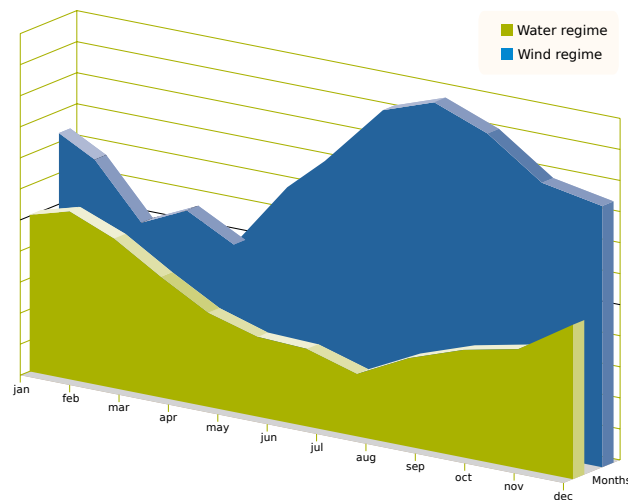


Source: ABEEólica, 2018

inertia. Thus, the system may experience stability problems during transients due to the high penetration of these machines (XIONG et al., 2019).

In order to maintain the electrical power system reliable, studies simulating various conditions must be performed beforehand, so the operators can be prepared for every occasion. These studies require mathematical models capable of adequately simulate the behaviour of every component on the grid. Particularly for wind power plants, an equivalent model is needed, since these facilities are usually largely spread and contain generators from different sizes and manufacturers.

Figure 3: Wind and water regime in the Brazilian Northeast Region



Source: ANEEL, 2005

## 1.2 Research Goals

The main goal of this research is to estimate parameters of an equivalent model of wind power plants. This will aid the studies concerning the system transient stability. To do so, an algorithm for parameter estimation will be developed combining two methods: Mean-Variance Mapping Optimization, an population-based heuristic approach, and Trajectory Sensitivity Method, a nonlinear approach. Also, as a secondary goal, a software, with graphical interface, for parameter estimation of nonlinear models will be developed.



## 2 MODELLING OF WIND TURBINE GENERATORS

With a growing share of energy covered by wind, system operators must consider how wind turbines affect the system stability during faults and maneuvers. To do so, mathematical models capable of describing these machines' behaviour are crucial. Obtaining these models, on the other hand, is not an easy task, due to considerable amount of wind turbines in large power plants, with different manufacturers, technologies, sizes, distances from point of connection and wind conditions. Thus, a model that describes well a particular turbine in a power plant, won't necessarily work for its neighboring generators. Also, due to industrial secrecy, manufacturers provide little or no information about how their turbines behave. Furthermore, having one model for every wind turbine within a power plant would result in a mathematical problem with high complexity and computational cost ([ERLICH et al., 2012](#)).

### 2.1 Generic Models of Wind Turbine Generators

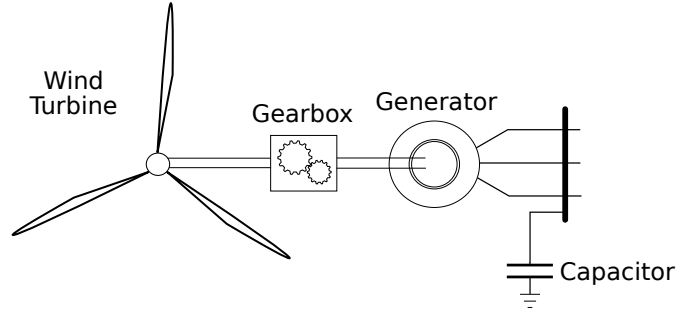
To address this problem, studies such as ([MULJADI; ELLIS, 2008](#)), ([ELLIS et al., 2011](#)), ([COUNCIL, 2008](#)) and ([ASMINE et al., 2011](#)), motivated specially by the Institute of Electrical and Electronics Engineers (IEEE) and the Western Electricity Coordinating Council (WECC), developed generic models able to predict the behaviour of entire wind power plants. Such models reduced the problem complexity, since they were composed of a single equivalent generator. A two-machine model is needed only in rare cases, such as when the wind power plant is composed of two or more types of wind turbines ([ELLIS et al., 2011](#)).

These studies have also shown that commercial wind turbine generators (WTG) could be sorted into four basic types, according to its technology ([ELLIS et al., 2011](#)). These types are described in the following subsections.

#### 2.1.1 Type-1 Wind Turbine Generator

The first type of wind turbine generator is composed of a Squirrel Cage Induction Generator (SCIG) connected to a wind turbine through a controlled gearbox, as displayed in Figure 4. Due to its torque-speed characteristics, generators of this type operate at constant rotor speed, requiring robust controllers on gearbox and blade. Besides, as usual to any induction generator, the SCIG absorbs reactive power during operation. Thus, capacitors are often employed for power factor correction purposes. Moreover, type-1 generators limit aerodynamic power by varying the pitch angle of their blades, imposing great mechanical stress on blades, shafts and gears, demanding a robust mechanical design and preventing these generators to operate above certain wind speed ([ELLIS et al., 2011](#)).

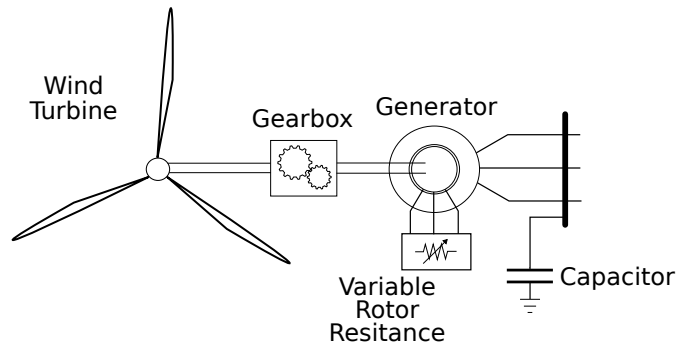
Figure 4: Representation of Type-1 Wind Turbine Generator



### 2.1.2 Type-2 Wind Turbine Generator

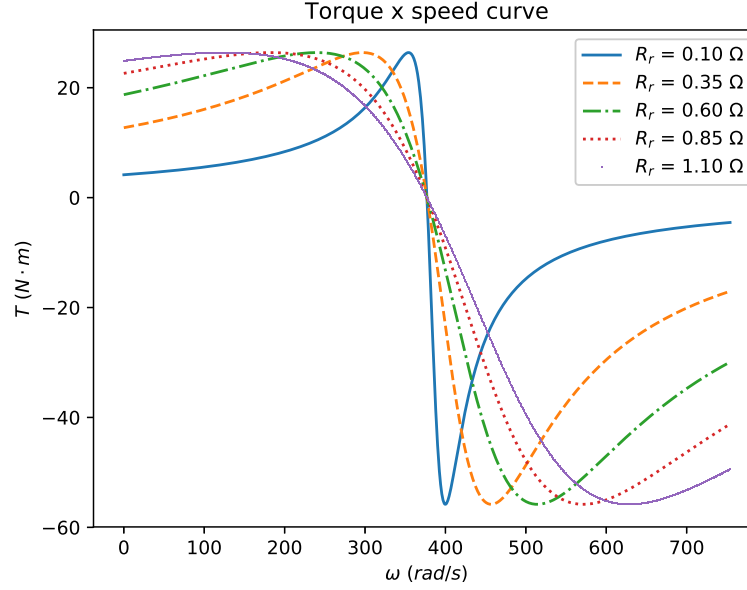
Similarly to Type-1 WTG, Type-2 Wind Turbine Generators are composed of an asynchronous machine connected to a wind turbine via gearbox, but, instead of SCIG, Wound Rotor Induction Generator (WRIG) are used to convert kinetic energy into electricity. The WRIG has access to its rotor windings, allowing to vary the rotor resistance. As a direct consequence, this machine can operate in different wind speeds by adjusting its torque-speed curve as needed ([ELLIS et al., 2011](#)). Therefore, Type-2 WTG have a WRIG with a variable resistance connected to its rotor terminals, as shown in Figure 5.

Figure 5: Representation of Type-2 Wind Turbine Generator



This type of generator has then three speed control systems, with rotor resistance control responding to rapid changes in speed, gearbox control for medium variations and pitch control for slow changes. These control system work together to maintain power output constant and reduce mechanical stress on components. The effects on the torque-speed curve caused by different rotor resistances are shown in Figure 6. For a fixed power, increasing rotor resistance increases the speed needed on the shaft, allowing the wind turbine to operate above rated wind speed. However, the speed range is only  $\pm 10\%$  of rated slip. Also, this machine still needs a reactive compensation circuit on its terminals ([MULJADI et al., 2010](#)).

Figure 6: Torque-speed curve



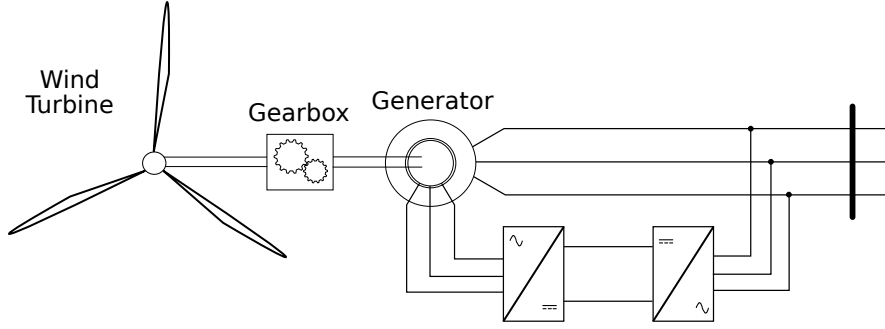
### 2.1.3 Type-3 Wind Turbine Generator

A Type-3 Wind Turbine Generator, often called Doubly Fed Induction Generator (DFIG), is also composed of a wound rotor machine connected to a wind turbine. But, instead of varying rotor resistance, a DFIG has its rotor supplied with AC voltage by a back-to-back frequency converter, as displayed in Figure 7. By varying the voltage frequency on the rotor circuit, the generator is able to supply power to the grid in a wider range of wind speed, reaching up to  $\pm 30\%$  of rated slip. In addition, the converter can control both real and reactive power independently, ending the necessity of capacitors (MULJADI et al., 2010). Since approximately 30% of rated power flows through the rotor windings, power electronics components have lower specifications and don't have great impact on overall costs. On the other hand, these generators need regular maintenance due to slip rings, brushes and gearbox, preventing its use in offshore applications (YARAMASU et al., 2015).

### 2.1.4 Type-4 Wind Turbine Generator

The last type of wind turbine generator, also called Full-Converter Generator, is composed of an electrical machine connected to the grid through a back-to-back frequency converter. The converter will operate converting the electrical frequency generated to standard, allowing this type of WTG to operate in a large range of wind speed (up to almost 100% of rated slip). Due to the converter operation, connection to the wind turbine can be made directly or via gearbox. Likewise, it allows the use of synchronous and asynchronous electrical machines as generator, with Permanent Magnet Synchronous

Figure 7: Representation of Type-3 Wind Turbine Generator



Generator (PMSG), Electrical Excited Synchronous Generator (EESG) and SCIG being most common, because of cost and maintenance purposes. Similar to DFIG, full-converter generators are able to control real and reactive power injected into the grid. However, since all power generated must flow through the power electronics, the overall cost of these generators is usually higher (YARAMASU et al., 2015). Figure 8 depicts a typical Type-4 Wind Turbine Generator.

Figure 8: Representation of Type-4 Wind Turbine Generator

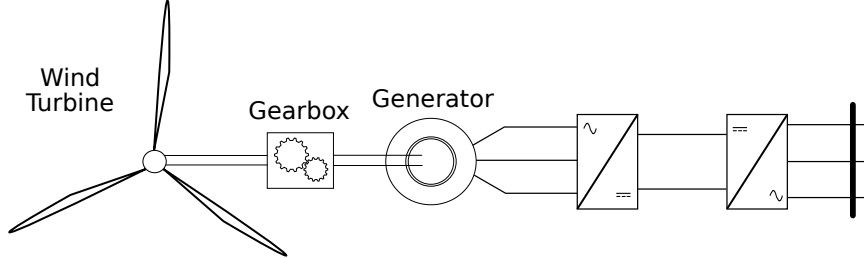


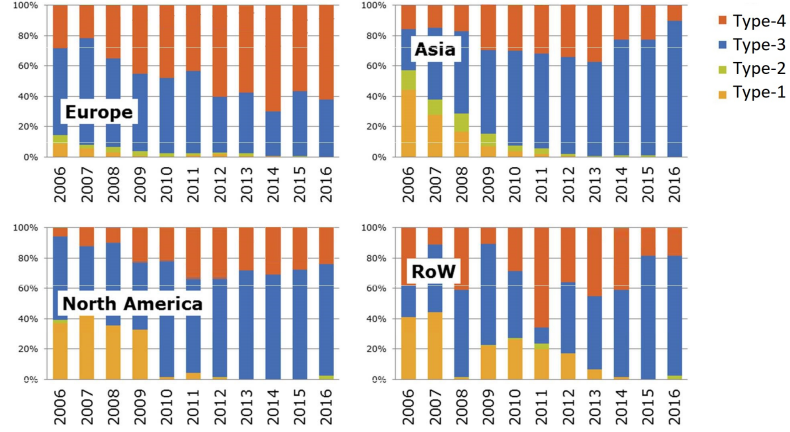
Figure 9 shows the evolution of share in installed capacity onshore for each generator type. The data shows how SCIG and WRIG lost space in the segment and how DFIG and Full-Converter Generators' participation rose, dominating the global market (MAGAGNA et al., 2017).

## 2.2 Model of Wind Turbine Generator Selected

Many mathematical models were developed during the last years that are able to represent Wind Turbine Generators of all types. All those models have in common the fact that they are based on the generic models proposed by the studies made by WECC and IEEE and presented in the last chapter.

Proposed by (ERLICH et al., 2012), this mathematical model is able to represent the dynamic of both Type-3 and -4 WTG's and can be used to simulate entire wind power

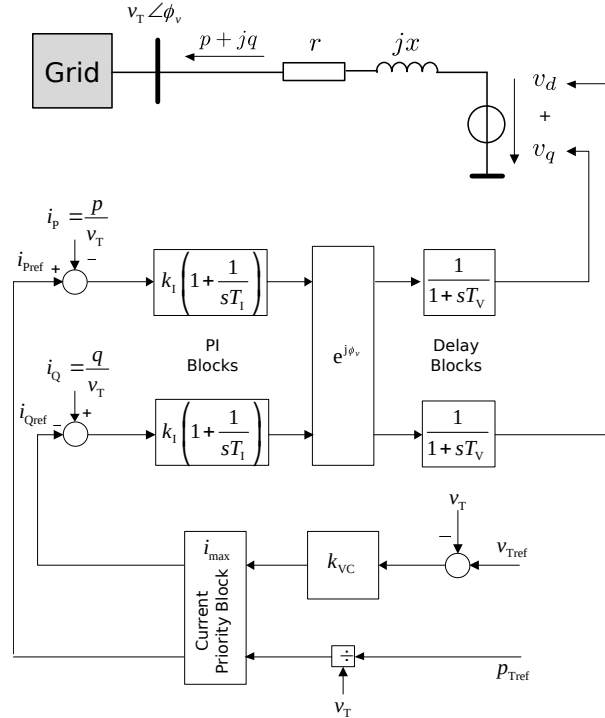
Figure 9: Share of installed capacity for each wind turbine generator type



Source: JRC

plants. In this model, a Thevenin equivalent circuit is connected to grid with a controlled voltage source, as depicted in Figure 10.

Figure 10: Type-3 WTG model proposed by Erlich



Source: Adapted from (ERLICH et al., 2012)

Terminal voltage  $v_T$  is the variable of interest in this model, appearing as input to DFIG's control system. Active and reactive current are calculated using that input,

according to equation (2.1).

$$\begin{cases} I_{Ac} = \frac{v_T}{p_{Tref}} \\ I_{Re} = k_{VC}(v_{Tref} - v_T) \end{cases} \quad (2.1)$$

The calculated currents feed a current priority block. This block analyses the current magnitude and terminal voltage level and decides whether power injection or voltage control will be prioritize. In summary, it checks if the generator's current is below a maximum level  $i_{max}$  and, if it is not, the block verifies if terminal voltage is above a threshold value  $v^*$  to decide what will be prioritized. The following algorithm describes the current priority block operation.

$$\begin{aligned} &\text{if } \sqrt{I_{Ac}^2 + I_{Re}^2} \leq i_{max} \text{ then:} \\ &\quad \begin{cases} i_{Pref} = I_{Ac} \\ i_{Qref} = I_{Re} \end{cases} \\ &\text{else:} \\ &\quad \text{if } v_T \geq v^* \text{ then:} \\ &\quad \quad \begin{cases} i_{Pref} = \min(i_{max}, I_{Ac}) \\ i_{Qref} = \sqrt{i_{max}^2 - i_{Pref}^2} \end{cases} \\ &\quad \text{else:} \\ &\quad \quad \begin{cases} i_{Qref} = \min(i_{max}, I_{Re}) \\ i_{Pref} = \sqrt{i_{max}^2 - i_{Qref}^2} \end{cases} \end{aligned}$$

The following PI blocks stand for the DFIG controllers (blade, gearbox, rotor-side and grid-side converters controllers) and their outputs follow the equations presented in (2.2).

$$\begin{cases} V_{PA} = k_I[(i_{Pref} - \frac{p}{v_T}) + \frac{1}{T_I} \int_0^t (i_{Pref} - \frac{p}{v_T}) dt] \\ V_{QA} = k_I[(\frac{q}{v_T} - i_{Qref}) + \frac{1}{T_I} \int_0^t (\frac{q}{v_T} - i_{Qref}) dt] \end{cases} \quad (2.2)$$

Until here the controller operates on terminal voltage oriented coordinates, so a coordinate transformation block is needed to adequate to synchronous grid coordinates. This block operates according to equations (2.3).

*In this chapter, a few mathematical models concerning Type-3WTG are presented and characterized and, at*

$$(2.3)$$

Last, two delay blocks supplying the voltage source (one for each component  $d$  and  $q$ ) simulate the delay effects of the electrical machine and the back-to-back converter. Their effects are described by (2.4).

$$\begin{cases} \dot{v}_d = \frac{1}{T_V}(v_d - V_{PAS}) \\ \dot{v}_q = \frac{1}{T_V}(v_q - V_{QAS}) \end{cases} \quad (2.4)$$

The outputs of this model are real and reactive power produced (or consumed) by the WTG and their equations are shown below.

$$\begin{cases} P_e = \frac{r(v_{Td}v_d + v_{Tq}v_q - v_T^2) + x(v_{Tq}v_d - v_{Td}v_q)}{r^2 + x^2} \\ Q_e = \frac{x(v_{Td}v_d + v_{Tq}v_q - v_T^2) - r(v_{Tq}v_d - v_{Td}v_q)}{r^2 + x^2} \end{cases} \quad (2.5)$$

Thus, this model can be interpreted as follows:

$$\begin{cases} \dot{x} = f(x, u, y, p) \\ y = g(x, u, y, p) \end{cases} \quad (2.6)$$

where the state variables  $x$ , inputs  $u$ , outputs  $y$  and parameters  $p$  vectors are described by (2.7), (2.8), (2.9) and (2.10), respectively.

$$x = [v_d, v_q]^T \quad (2.7)$$

$$u = [v_T, \theta_v, P, Q]^T \quad (2.8)$$

$$y = [P_e, Q_e]^T \quad (2.9)$$

$$p = [r, x, k_I, T_I, T_V, k_{VC}]^T \quad (2.10)$$

In (2.10), the parameters correspond to the stator equivalent resistance  $r$  and reactance  $x$ , PI gain  $k_I$  and time constant  $T_I$ , delay block time constant  $T_V$  and voltage block gain  $k_{VC}$ .





### 3 PARAMETER ESTIMATION PROCESS

Parameter estimation problems can be interpreted as optimization problems, where one must find the optimal values of parameters in order to reduce the error between real system and model. During the years, many methods were developed to address this problem, but two approaches have been largely employed to obtain its solution.

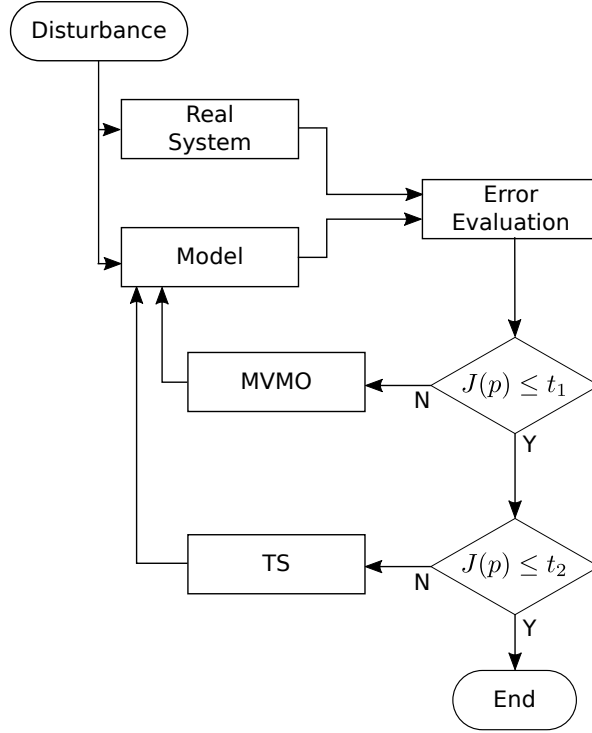
The first approach applies metaheuristics to obtain a sufficiently good solution. These methods are used in a variety of cases, ranging from biological to engineering problems, due to the fact that they are not developed for a specific type of problem. Metaheuristics employ a stochastic search to encounter (near-)optimal solutions within a given region. However, they often take a great amount of time to converge to a solution (BLUM; ROLI, 2003). Examples of metaheuristics are Ant Colony Optimization, Differential Evolution, Particle Swarm Optimization and Genetic Algorithm. Applications of this approach in electrical power system cases can be found in (TODOROVSKI; RAJIČIĆ, 2006) and (YOSHIDA et al., 2000).

The second approach applies analytical methods to find a global/local optimum solution. These methods use equations derived from the problem to locate an optimal solution. Thus, they are problem specific and must be adapted from one case to another. Analytical methods often converge in few iterations, reducing processing time, but are sensitive to initial conditions.

In this work is proposed to combine both approaches, reducing the effects of their disadvantages and improving overall convergence. Mean-Variance Mapping Optimization (MVMO) was the metaheuristic chosen for this problem, alongside Trajectory Sensitivity Method (TSM) as analytical method. Both methods will be discussed in the following sections.

The flowchart depicted in Figure 11 illustrates how the proposed method works. At first, a disturbance occurs, resulting in a dynamic response of the real system. The real system's outputs are compared to the model behaviour when the same disturbance is applied to it. The error  $J(p)$  is evaluated and while it is greater than a given tolerance  $tol_1$ , MVMO algorithm will search for a local solution. Afterwards, the error will eventually drop to a value lower than  $tol_1$ , and TSM will be used to refine the search to a optimal solution, with error level below tolerance  $tol_2$ . The error will be evaluated through the Least-Squares Method, given by equation 3.1, where  $y_r$  and  $y$  stand for the real system

Figure 11: Flowchart of estimation method



and model outputs.

$$J(p) = \frac{1}{2} \int_0^{T_0} (y_r(t) - y(t))^T (y_r(t) - y(t)) dt \quad (3.1)$$

### 3.1 Mean-Variance Mapping Optimization

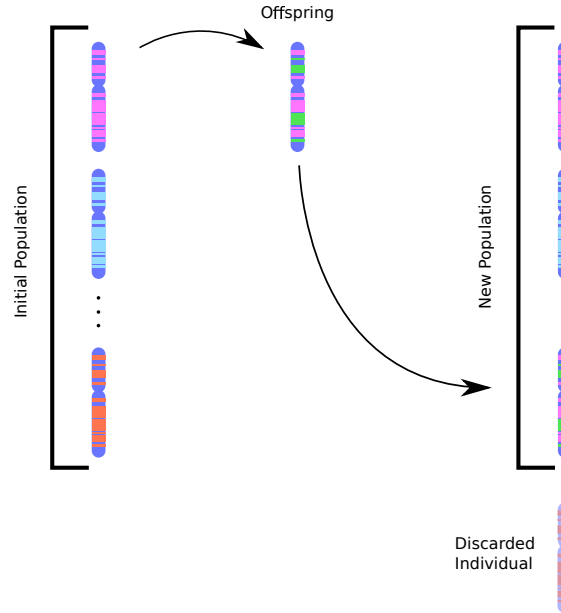
Presented in (ERLICH; VENAYAGAMOORTHY; WORAWAT, 2010), this population-based metaheuristic shares characteristics with other evolutionary algorithms, but differ from them on how to induce mutations on the offspring in order to diversify the population. By considering statistical data of population during mutation process, MVMO introduces a memory factor to it, enhancing search mechanism. Due this factor, MVMO performs better than similar metaheuristics when population size is relatively small (NAKAWIRO; ERLICH; RUEDA, 2011). The terms ‘gene’, ‘individuals’ and ‘population’ refer to ‘parameter’, ‘parameter vector’ and ‘set of parameter vectors’ in MVMO, for the sake of analogy.

Before starting the parameter search process, a few settings must be done, such as population size, number of offspring, number of genes selected for mutation and selection method. Also, the search region is defined by setting the range within genes can vary. This constrains the parameters values within a feasible region, preventing divergence. The

search region is later normalized for all genes, aiding the process. Termination criteria is also set in this step. In this work, both number of generations and error will be used as stop criteria.

After that, a randomly-distributed population is generated, evaluated and sorted. Moreover, the mean and variance of every gene in each population are calculated. These values will later be used on the mutation process. The individual with lower error is selected as parent from whom a new individual will be generated. The offspring is then created following three steps common in evolutionary algorithms: gene selection, mutation and crossover. After creation, the offspring is introduced to the population and the worst individual is discarded, as depicted in Figure 12.

Figure 12: Exemplification of MVMO process



**Gene selection** can be done in many ways and even vary throughout the estimation process, with strategies' efficiency depending on the problem. However, three strategies are commonly used in this step. The first one is comprised of randomly selecting which genes will suffer mutation and which will be directly inherited from the parent. Gene selection can also be done by a moving window approach or even a combination of both strategies, with part of the genes selected at random and other through the window.

**Mutation** step takes place right after gene selection. At first, each selected gene receives a random value  $x'_i$  between  $[0,1]$  that will be used as an input to a mapping function based on the mean and variance of each particular gene on the population. Variance  $v_i$  will directly influence on the shape factor given by (3.2), where  $f_s$  is the scaling factor responsible for focusing on exploration or exploitation. In the event of zero variance, the

last non-null value of  $v_i$  is used.

$$s_i = -f_s \ln(v_i) \quad (3.2)$$

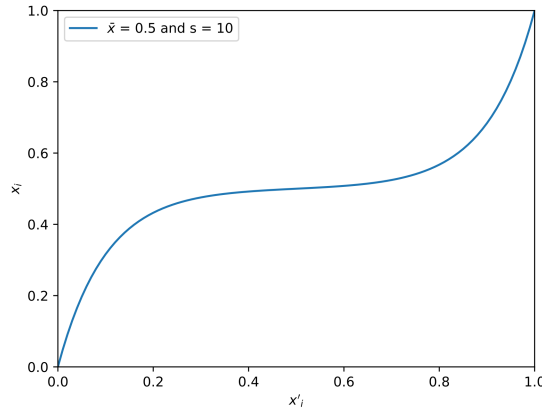
Shape factor and mean value of genes of the population are used as inputs to a transformation function  $h$ , detailed in (3.3). The final value of the gene is obtained through the mapping function described by equation (3.4), where  $h_x = h(u_i = x'_i)$ ,  $h_1 = h(u_i = 1)$  and  $h_0 = h(u_i = 0)$ . It is important to notice that the mapping function will always provide a result in the interval  $[0,1]$ , not violating the normalization made at beginning.

$$h(\bar{x}_i, s_{i1}, s_{i2}, u_i) = \bar{x}_i(1 - e^{-u_i s_{i1}}) + (1 + \bar{x}_i)e^{-(1-u_i)s_{i2}} \quad (3.3)$$

$$x_i = h_x + (1 - h_1 + h_0)x'_i - h_0 \quad (3.4)$$

The resulting mapping function is depicted in Figure 13. The effects of different mean and shape factor values can be observed on Figure 14.

Figure 13: Example of MVMO mapping function



As shown in (3.3), two shape factors are used to evaluate the function. Different values of shape factors emphasizes the search below or above mean value. Thus, by controlling the values  $s_{i1}$  and  $s_{i2}$ , the method can prioritize exploitation (global search) or exploration (local search) on a given region. Figure 15 depicts how asymmetrical shape factors affect the mapping function.

The final step during offspring generation is crossover. During this phase, the mutated genes are united with the remaining genes inherited from parent, forming the new individual. This new individual is evaluated and included to the population if it is better than, at least, the population's worst individual. This process goes on until at least one stop criterion has been fulfilled.

Figure 14: Effect of different mean and shape factor values on the mapping function

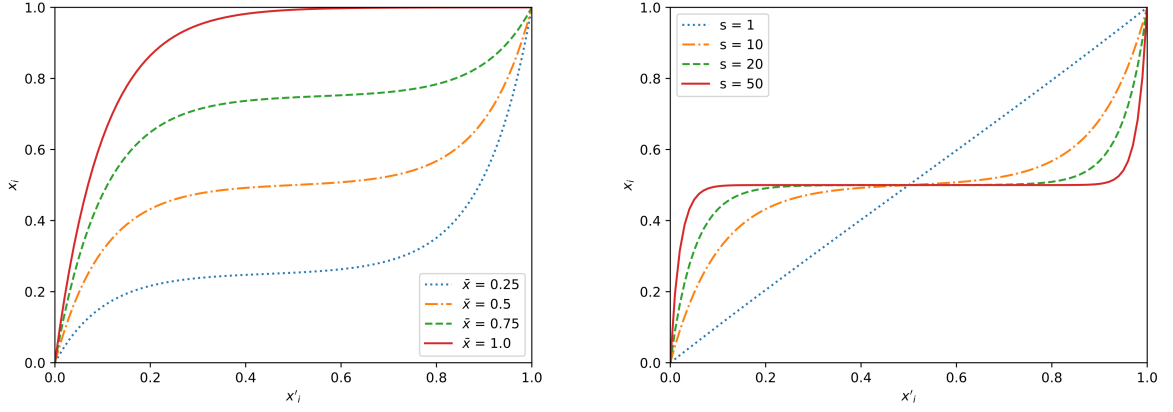
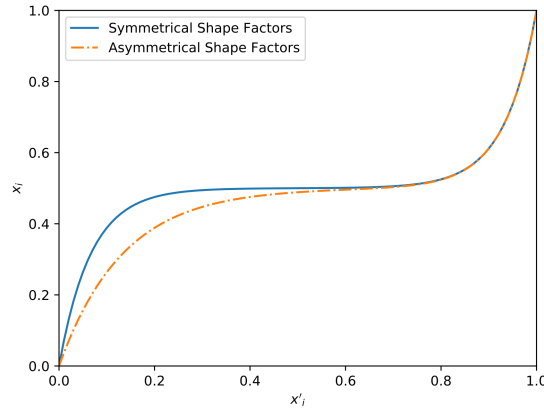


Figure 15: Comparison between symmetrical and asymmetrical shape factors



The main advantages of this method are low computational cost, good performance using small populations, constrained search region, preventing divergence, and the fact that it is non-specific. On the other hand, this method, as other metaheuristics, takes a great amount of time to converge when its error approaches zero.

### 3.2 Trajectory Sensitivity Method

Considering a nonlinear system described by (2.6), in order to minimize the error between model and real system, given by (3.1), one must discover a parameter vector  $p^*$  such as:

$$G(p^*) = \frac{\partial J(p^*)}{\partial p} = 0 \quad (3.5)$$

Truncating the Taylor series for  $G(p)$  on the first-order term results on (3.6). The variable  $\Gamma$  is described in (3.7).

$$G(p^*) = G(p) + \Gamma(p)(p^* - p) \quad (3.6)$$

$$\Gamma(p) = \frac{\partial G}{\partial p} \approx \int_0^{T_0} \left( \frac{dy}{dp} \right)^T \left( \frac{dy}{dp} \right) dt \quad (3.7)$$

By rearranging the terms on (3.6), the following equation is obtained. It describes how the parameters are updated after the  $n^{th}$  iteration.

$$p^{n+1} = p^n + \Gamma^{-1}(p^n) \cdot G(p^n) \quad (3.8)$$

The partial derivatives (also called trajectory sensitivities)  $\frac{\partial y}{\partial p}$ , used directly in (3.7) and indirectly in (3.5), can be approximated by the difference shown in (3.9). The outputs  $y^1$  and  $y^0$  are obtained using parameter vectors  $p^1$  and  $p^0$ , respectively, and  $\Delta p = p^1 - p^0$ . Using (3.9) allows Trajectory Sensitivity method to be applied on both differentiable and non-differentiable systems (BENCHLUCH; CHOW, 1993), (CARI; ALBERTO; BRETAS, 2006).

$$\frac{\partial y}{\partial p} \approx \frac{y^1 - y^0}{\Delta p} \quad (3.9)$$

The Trajectory Sensitivity Method has fast convergence characteristics and can be applied directly to nonlinear problems, not requiring linearization. Also, by analyzing the sensitivities, the method provides information about parameters' identifiability. However, TSM is very sensitive to initial value of parameter chosen as starting point. Thus, if the initial values are too far from the real values, the method can either diverge or converge to wrong values. Besides, the information provided to the method must contain the effects of the parameters, otherwise they won't be observable (BENCHLUCH; CHOW, 1993).

By associating MVMO and TSM, the hybrid estimation approach proposed in this work combines most benefits of both methods whilst mitigating their disadvantages. The resulting method has smaller convergence time when compared to MVMO alone and is less sensitive to initial values of parameters than TSM.

## 4 SOFTWARE CONCEPT

In this chapter, the concept behind the software in development is presented. The entire software will be developed using Python, a powerful, simple and fast high-level programming language that has gained large space in various sectors of industry and academy. Its rise is due mainly to the enormous number of libraries and forums developed and maintained by the users. Some examples of libraries used in this project are numpy (for scientific computing), matplotlib (plotting library), Tkinter and Qt (Graphical User Interface toolkit). Python is also open-source, not requiring a paid software to code and most of its applications are free.

Although this project focus on using specific estimation methods and mathematical model for the DFIG problem, the software in development will not be specific to them. Instead, it will be generic and both model and method can be imported as packages. This will allow future users to use this application on different problems concerning parameter estimation. Also, comparison between method's performance and model's precision can be easily done with this software.

In order to improve the experience of users, a Graphical User Interface (GUI) will be developed. It will provide an simple environment for all users, so they won't need to go through the code to change any settings. Instead, the settings will be done at the beginning of the process and follow a predefined order.

The start page will display some information about the software and the parameter estimation process. Next, the user will choose from a list which mathematical model will be employed. After that, a list of identification methods will be presented and the user will be able to pick up to two methods. The settings of the chosen methods will done on the following windows and, finally, the user will enter the file containing the real system data and point out which data will be used as inputs and outputs. With all set, the estimation process will start and, at its end, a report will display the estimated parameters and the comparison between real system and model behaviours.

The order presented is not definitive and may change throughout the project if needed. However, all the steps discussed are core to the estimation process and cannot be discarded. Also, some other steps may be included in order to improve the software performance.





## 5 EXPECTED RESULTS

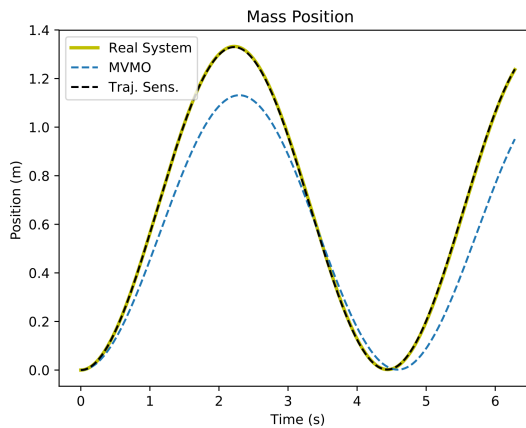
The expected result of this work is a software capable of correctly estimating the parameters of Type-3 WTG's mathematical model. To do so, the software will apply the proposed estimation method comprises of MVMO and TSM methods combined.

The measurements will be obtained from a small power system simulated on specific software, such as Digsilent or MATLAB. At first, the model proposed in (ERLICH et al., 2012) will be employed, but it can be further changed if needed. Also, other estimation methods, such as Particle Swarm Optimization, Differential Evolution or Kalman Filters, may be implemented for comparison purposes.

### 5.1 Partial Results

The hybrid approach for parameters estimation presented in this work is already implemented and have shown great results for models. As depicted in Figure 16, the proposed method can correctly identify the parameters of a spring-mass system. The same application was employed on load model identification and is subject of a paper presented by the author on the 2019 Canadian Conference on Electrical and Computer Engineering.

Figure 16: Results of method for spring-mass system



### 5.2 Work Progress

With the methods already implemented and tested, the focus now is on the DFIG model. The model has presented some results, but it is not accurate as required, requesting some studies about this topic. Also, the GUI is under development and already has some features implemented using Python's library Tkinter. A proposal to also develop features using Qt, a different GUI tool package, is currently under consideration.



## BIBLIOGRAPHY

- ABEEOLICA. **Annual Wind Energy Report**. Sao Paulo, 2018.
- AMARANTE, O. A. C. do et al. **Atlas do Potencial Eólico Brasileiro**. Brasilia, 2001.
- ANEEL. **Atlas de Energia Elétrica do Brasil**. Brasilia, 2005. Disponível em: [http://www.aneel.gov.br/livros/-/asset{\\_}publisher/eZ674TKh9oF0/content/atlas-de-energia-eletrica-do-brasil/656](http://www.aneel.gov.br/livros/-/asset{_}publisher/eZ674TKh9oF0/content/atlas-de-energia-eletrica-do-brasil/656).
- ASMINE, M. et al. Model Validation for Wind Turbine Generator Models. **Power Systems, IEEE Transactions on**, v. 26, n. 3, p. 1769–1782, 2011. ISSN 0885-8950.
- BENCHLUCH, S. M.; CHOW, J. H. A Trajectory Sensitivity Method for the Identification of Nonlinear Excitation System Models. **IEEE Transactions on Energy Conversion**, v. 8, n. 2, p. 159–164, jun 1993. ISSN 15580059. Disponível em: <http://ieeexplore.ieee.org/document/222699/>.
- BLUM, C.; ROLI, A. Metaheuristics in Combinatorial Optimization: Overview and Conceptual Comparison. **ACM Computing Surveys**, v. 35, n. 3, p. 268–308, sep 2003. ISSN 0360-0300. Disponível em: <http://portal.acm.org/citation.cfm?doid=937503.937505>.
- CARI, E. P.; ALBERTO, L. F.; BRETAS, N. G. A methodology for parameter estimation of synchronous generators based on trajectory sensitivity and synchronization technique. In: **2006 IEEE Power Engineering Society General Meeting, PES**. IEEE, 2006. p. 6 pp. ISBN 1424404932. Disponível em: <http://ieeexplore.ieee.org/document/1709492/>.
- Commission European. **A strategy for smart, sustainable and inclusive growth**. Brussels, 2010. 1–37 p. Disponível em: <https://www.eea.europa.eu/policy-documents/com-2010-2020-europe-2020>.
- COUNCIL, W. E. C. Wecc wind power plant power flow modeling guide. **WECC Wind Generator Modeling Group, Tech. Rep**, 2008.
- ELLIS, A. et al. Generic models for simulation of wind power plants in bulk system planning studies. **IEEE Power and Energy Society General Meeting**, p. 1–8, 2011. ISSN 19449925.
- EPE. **Anuário Estatístico de Energia Elétrica 2018 no ano base de 2017**. Rio de Janeiro, 2018. 249 p. Disponível em: <http://www.epe.gov.br/sites-pt/publicacoes-dados-abertos/publicacoes/PublicacoesArquivos/publicacao-160/topico-168/Anuario2018vf.pdf>.
- ERLICH, I. et al. Determination of Dynamic Wind Farm Equivalents using Heuristic Optimization. **Power and Energy Society General Meeting, IEEE**, p. 1–8, 2012.
- ERLICH, I.; VENAYAGAMOORTHY, G. K.; WORAWAT, N. A Mean-Variance Optimization algorithm. **2010 IEEE World Congress on Computational Intelligence, WCCI 2010 - 2010 IEEE Congress on Evolutionary Computation, CEC 2010**, n. February, p. 1–6, 2010.

Federative Republic of Brazil. **Lei 10438/2002**. Brasilia: [s.n.], 2002. 1–21 p.  
Disponível em: [http://www.planalto.gov.br/ccivil/\\_03/leis/2002/L10438.htm](http://www.planalto.gov.br/ccivil/_03/leis/2002/L10438.htm)[http://www.planalto.gov.br/ccivil/\\_03/LEIS/2002/L104](http://www.planalto.gov.br/ccivil/_03/LEIS/2002/L104)>.

MAGAGNA, D. et al. **Supply chain of renewable energy technologies in Europe: An analysis for wind, geothermal and ocean energy**. [s.n.], 2017. ISSN 1831-9424. ISBN 978-92-79-74281-1. Disponível em: <https://ec.europa.eu/jrc/en/publication/eur-scientific-and-technical-research-reports/supply-chain-renewable-energy-technologies-europe-analysis-wind-geothermal-and-ocean-energy>>.

MULJADI, E.; ELLIS, A. Validation of wind power plant models. **IEEE Power and Energy Society 2008 General Meeting: Conversion and Delivery of Electrical Energy in the 21st Century, PES**, p. 1–7, 2008. ISSN 1932-5517.

MULJADI, E. et al. Short circuit current contribution for different wind turbine generator types. In: **IEEE PES General Meeting, PES 2010**. IEEE, 2010. p. 1–8. ISBN 9781424483570. Disponível em: <http://ieeexplore.ieee.org/document/5589677/>>.

NAKAWIRO, W.; ERLICH, I.; RUEDA, J. L. A novel optimization algorithm for optimal reactive power dispatch: A comparative study. **2011 4th International Conference on Electric Utility Deregulation and Restructuring and Power Technologies (DRPT)**, n. 1, p. 1555–1561, 2011. ISSN 0278-0046. Disponível em: <http://ieeexplore.ieee.org/document/5994144/>>.

TODOROVSKI, M.; RAJIČIĆ, D. An initialization procedure in solving optimal power flow by genetic algorithm. **IEEE Transactions on Power Systems**, v. 21, n. 2, p. 480–487, 2006. ISSN 08858950.

Wind Europe. Wind energy in Europe in 2018: Trends and statistics. **Wind Europe. (2019). Wind energy in Europe in 2018: Trends and statistics.**, 2019. ISSN 0309524X.

XIONG, L. et al. Stability Enhancement of Power Systems With High DFIG-Wind Turbine Penetration via Virtual Inertia Planning. **IEEE Transactions on Power Systems**, v. 34, n. 2, p. 1352–1361, mar 2019. ISSN 0885-8950. Disponível em: <https://ieeexplore.ieee.org/document/8463592/>>.

YARAMASU, V. et al. High-power wind energy conversion systems: State-of-the-art and emerging technologies. **Proceedings of the IEEE**, v. 103, n. 5, p. 740–788, may 2015. ISSN 00189219. Disponível em: <http://ieeexplore.ieee.org/document/7109820/>>.

YOSHIDA, H. et al. A Particle swarm optimization for reactive power and voltage control considering voltage security assessment. **IEEE Transactions on Power Systems**, 2000. ISSN 08858950.